

Quantum Control of Interacting Bosons in Periodic Optical Lattice

Analabha Roy and L.E. Reichl
Center for Complex Quantum Systems
and

Department of Physics
The University of Texas at Austin, Austin, Texas 78712

April 2, 2024

Abstract

We study the avoided crossings in the dynamics of quantum controlled excitations for an interacting two-boson system in an optical lattice. Specifically, we perform numerical simulations of quantum control in this system where driving pulses connect the undriven stationary states in a manner characteristic of Stimulated Raman Adiabatic Passage (STIRAP). We demonstrate that the dynamics of such a transition is affected by chaos induced avoided crossings, resulting in a loss in coherence of the final outcome in the adiabatic limit.

1 Introduction

Stimulated Raman Adiabatic Passage, or STIRAP, is a well-known method of inducing coherent excitations of quantum systems from the ground state to states with higher energy. This is achieved using coherent time-modulated laser fields that result in complete population transfer from an initially populated ground state to a target state via an intermediate state. STIRAP was first proposed by Hioe and coworkers [1], [2]. A crucial preliminary work by Becker et al. [3] achieved efficient vibrational excitation by using a molecular beam as an optically pumped active medium and led to the development of the STIRAP concept. The theoretical work was formulated by Kuklinsky, Gaubatz, Hioe and Bergmann shortly thereafter [4]. STIRAP was further confirmed by manipulating the vibrational and rotational degrees of freedom in sodium dimers [5].

Since then, STIRAP has been used to control transitions in a diverse range of matter-optics systems [6], ranging from molecular alignment [7], and molecular rotation [8], to the coherent acceleration of ultracold atom systems by transfer between a stationary and a moving optical lattice [9], and controlled dipole

excitations in ultracold bosons subjected to radiation induced double well potentials [10]. In the latter two cases, STIRAP has also been used to illustrate the influence of the underlying classical chaos in the atom dynamics by looking at avoided crossings in the Floquet eigenphase spectrum. The exact procedure was first described by Na and Reichl [11] for a driven single particle in a box.

Optical lattice systems have been of great interest in experimental physics [12] and [13]) and theoretical physics [14], [15] for some time. In 1992, Graham, Schlautmann and Zoller showed that the center of mass motion of cold atoms in an optical lattice could be decoupled from their internal degrees of freedom [16]. Since then, the influence of chaos in optical lattice systems has been an important factor in the manipulation of such systems [9], [17]. Number squeezing and subpoissonian distribution of atoms in each site in an optical lattice have been reported by Itah et al. [18]. The system of interest in our work is an optical lattice with a 2-periodic boundary condition that traps two interacting bosons. We seek to use this system as a test case for larger many-particle problems, where the Hilbert space can be restricted to the subspace of all N -periodic wavefunctions, with large N . Here, we set N to the lowest meaningful value of 2, since singly periodic wavefunctions do not take into account the probability of two particles being in separate wells of the lattice. Furthermore, Fernholtz et al. [19] have recently shown that it is possible to trap a cold atomic system on the surface of a toroid and to achieve a two-dimensional periodic potential similar to the ringed optical lattice that we shall consider in this work.

In subsequent sections, we consider the application of STIRAP to an interacting boson system confined to a one-dimensional optical lattice with periodic boundary conditions. A linear version of our system has been implemented in experimental studies [20] using ultra-cold atoms. In section 2, we derive an expression for the basic model and we discuss the numerical methods used to obtain the stationary eigenstates for this system. In section 3, we discuss the process by which coherent transitions between selected symmetrized energy eigenstates can be achieved for this system. We will also show that avoided crossings in the Floquet states can be associated with real transitions of the undriven symmetrized eigenstates. Concluding remarks are made in section 4.

2 The Basic Model

Our system consists of two atoms (bosons), each of mass m , confined to a spatially periodic optical lattice of radius ρ . The dipole interaction between the atom and the optical lattice gives us the atomic Hamiltonian

$$H = \frac{L_1^2}{2I} + \frac{L_2^2}{2I} + \kappa_0[\cos(2\theta_1) + \cos(2\theta_2)] + u_0\delta(\theta_1 - \theta_2), \quad (1)$$

where $I = m\rho^2$, L_i and θ_i are the angular momentum and angle, respectively, of the i th particle ($i = 1, 2$), κ_0 is the lattice amplitude, and u_0 is the strength of the point contact pseudopotential interaction between the bosons.

It is useful to write the Hamiltonian in terms of dimensionless parameters (L'_i, θ'_i). For particles interacting with the optical lattice in Eq. (1), the angular momentum transfer occurs in discrete units $\Delta L = 2\hbar$. We therefore define $L'_i = \frac{L_i}{2\hbar}$, and $\theta'_i = 2\theta_i$. Thus, $H'_i = \frac{H}{4\hbar\omega_r}$, $\kappa' = \frac{\kappa}{4\hbar\omega_r}$, $u'_0 = \frac{u_0}{2\hbar\omega_r}$ and $t' = 4\omega_r t$, where $\omega_r = \frac{\hbar}{2I}$ is the recoil frequency. We also scale all other frequencies as $\omega' = \frac{\omega}{4\omega_r}$. We then drop the primes on the dimensionless parameters and obtain the dimensionless Hamiltonian

$$H_0 = L_1^2 + L_2^2 + \kappa_0[\cos\theta_1 + \cos\theta_2] + u_0\delta(\theta_1 - \theta_2). \quad (2)$$

We use as a basis set, the eigenstates of the angular momentum operator $\hat{L}|n\rangle = n|n\rangle$ or $\langle\theta|n\rangle = \frac{1}{\sqrt{2\pi}}e^{in\theta}$ where integers n range over the values $-\infty \leq n \leq \infty$.

We numerically diagonalize the Hamiltonian in Eq. (2) using a nonadaptive finite element method. The 2-particle boson states are obtained by taking symmetrized products of single particle states:

$$\langle\theta_1, \theta_2|n_1, n_2\rangle^{(s)} = \frac{1}{\sqrt{2}}[\langle\theta_1|n_1\rangle\langle\theta_2|n_2\rangle + \langle\theta_1|n_2\rangle\langle\theta_2|n_1\rangle]. \quad (3)$$

These states are then used to create a Hamiltonian matrix from Eq. (2). The eigenvalues E_α and eigenvectors $|E_\alpha\rangle$ of the Hamiltonian matrix were determined numerically using the appropriate subroutine for diagonalizing real symmetric matrices in the GNU Scientific Library [21]. Figure 1.a shows the energy levels E_1 through E_{66} . Figure 1.b gives of magnified view of these levels. Figures 2.a through 2.e are the probability distribution plots for the states $\langle\theta_1, \theta_2|E_1\rangle$, $\langle\theta_1, \theta_2|E_3\rangle$, $\langle\theta_1, \theta_2|E_4\rangle$, $\langle\theta_1, \theta_2|E_5\rangle$, and $\langle\theta_1, \theta_2|E_{15}\rangle$ respectively at the value $\kappa_0 = 7.287781$, the lattice amplitude we use in subsequent sections. We chose these states because they have the largest coupling $\langle E_{\alpha'}|\cos(\theta_i)|E_\alpha\rangle$ and lead to robust STIRAP transitions.

3 Induced Transitions in the Interacting System

Our goal will be to transition the bosons from the ground state $|E_1\rangle$ of the optical lattice to the state $|E_{15}\rangle$, using $|E_4\rangle$ as the intermediate state. We will accomplish this by perturbing the system with two Gaussian shaped radiation pulses, the first pulse with carrier frequency $\omega_f = E_{15} - E_4$ and the second pulse with carrier frequency $\omega_s = E_4 - E_1$. In the presence of these pulses, the Hamiltonian takes the form

$$H(t) = L_1^2 + L_2^2 + \kappa(t)[\cos\theta_1 + \cos\theta_2] + u_0\delta(\theta_1 - \theta_2), \quad (4)$$

where

$$\kappa(t) = \kappa_0 + \lambda_f(t)\cos(\omega_f t) + \lambda_s(t)\cos(\omega_s t). \quad (5)$$

Here, the Gaussian amplitudes $\lambda_f(t) = \lambda_0\exp[-(t - t_f^o)^2/4t_d^2]$ and $\lambda_s(t) = \lambda_0\exp[-(t - t_s^o)^2/4t_d^2]$.

As shown in references [8], [9], [10] and [11], it is possible to use Floquet theory to analyze the effect of the radiation pulses on the system as they pass through the system. The only requirement is that the pulse envelopes $\lambda_f(t)$ and $\lambda_s(t)$ be slowly varying compared to the carrier wave periods $2\pi/\omega_f$ and $2\pi/\omega_s$, respectively. We can then break the time evolution into N narrow time windows, the k th window centered at a time $t = t_{fix}^k$. In the k th time window we can write the Hamiltonian in the form

$$H(t; t_{fix}^k) = L_1^2 + L_2^2 + \kappa(t; t_{fix}^k)[\cos \theta_1 + \cos \theta_2] + u_0 \delta(\theta_1 - \theta_2). \quad (6)$$

The Hamiltonian $H(t; t_{fix}^k)$ for the k th time window is time-periodic if ω_f and ω_s are commensurate and we can use Floquet theory to analyze the behavior of the system in that time window. The value $\kappa_0 = 7.287781$ was chosen to achieve the commensurability $\omega_f/\omega_s = 3/2$, with $\omega_f = 10.896058668420753$.

The period of the Hamiltonian $H(t; t_{fix}^k)$ is then given by $T = \pi \left(\frac{3}{\omega_f} + \frac{2}{\omega_s} \right)$.

The Floquet Hamiltonian, for the k th time window, is given by $H_F^k(t) = H(t; t_{fix}^k) - i \frac{\partial}{\partial t}$ (in dimensionless units). $H_F^k(t)$ is Hermitian and has eigenvalues Ω_ν and eigenvectors $|\phi_\nu(t)\rangle$. The eigenvalues are defined modulo $2\pi/T$ and the eigenvectors are time-periodic with period T . The quantum state $|\psi^k(t)\rangle$, which is a solution to the Schrödinger equation $i \frac{\partial |\psi^k(t)\rangle}{\partial t} = H(t; t_{fix}^k) |\psi^k(t)\rangle$ can be expanded in a spectral decomposition

$$|\psi(t)\rangle = \sum_{\nu} A_{\nu} e^{-i\Omega_{\nu}t} |\phi_{\nu}(t)\rangle, \quad (7)$$

where A_{ν} gives the contribution of the ν th Floquet state to the evolution of the system in a given time-window. The Floquet evolution operator, $U_F(T)$, in the basis of symmetrized 2-boson states $|n\rangle \equiv |n_1, n_2\rangle^{(s)}$ (see Eq. 3), is given by

$$\langle n | U_F(T) | m \rangle = \sum_{\nu} e^{-i\Omega_{\nu}T} \langle n | \phi_{\nu}(0) \rangle \langle \phi_{\nu}(0) | m \rangle. \quad (8)$$

The Floquet evolution matrix is constructed as follows. To obtain the m th column of $\langle n | U_F(T) | m \rangle$, choose initial conditions $\langle m' | \psi(0) \rangle = \delta_{m',m}$ and integrate the Schrödinger equation from time $t = 0$ to time $t = T$. The state at time $t = T$ is the m th column of the Floquet evolution matrix. For our system, the integration was done using an 8th order Runge-Kutta Prince Dormand algorithm [22] from the GNU Scientific Library [21], and the Floquet evolution matrix was diagonalized using a parallelized LAPACK library through the Scalable Library for Eigenvalue Problem Computations (Slepc) [23]. The eigenvalues, $e^{-i\Omega_{\nu}T}$ can be used to obtain Ω_{ν} . We obtained the Floquet eigenvalues and eigenvectors for each time window. The eigenstates in neighboring time windows will be approximately orthonormal and we can use this fact to follow each Floquet eigenstate and eigenvalue as the pulses move through the system.

We chose the following parameters for the Gaussian pulses; $\lambda_0 = 0.2$, $t_f = (1/3)t_{tot}$, $t_s = (2/3)t_{tot}$, and $t_d = (1/14)t_{tot}$. Here t_{tot} defines the total time scale for both pulses, and t_{fix} is expressed in units of t_{tot} unless otherwise stated.

Figure 3 shows the Floquet eigenvalues of the relevant Floquet eigenstates as the system evolves in adiabatic time t_{fix} . The relevant eigenstates are the ones isomorphic to the states connected by the STIRAP pulses viz. $|E_1\rangle$, $|E_4\rangle$, and $|E_{15}\rangle$. We notice that the Floquet eigenvalues are degenerate at $t_{fix} = 0$ and $t_{fix} = t_{tot}$ as expected. The Floquet states and corresponding eigenvalues are labeled alphabetically as follows:

1. The eigenphase whose corresponding Floquet eigenstate is supported by the undriven state $\frac{1}{\sqrt{2}} [|E_4\rangle - |E_{15}\rangle]$ at $t_{fix} = 0$ is labeled as Ω_B and the Floquet eigenstate as $|\phi_B\rangle$.
2. The eigenphase whose corresponding Floquet eigenstate is supported by the undriven state $\frac{1}{\sqrt{2}} [|E_4\rangle + |E_{15}\rangle]$ at $t_{fix} = 0$ is labeled as Ω_C and the Floquet eigenstate as $|\phi_C\rangle$.
3. The eigenphase whose corresponding Floquet eigenstate is supported by the undriven ground state $|E_1\rangle$ at $t_{fix} = 0$ is labeled as Ω_D and the Floquet eigenstate as $|\phi_D\rangle$.

The evolution of the Floquet eigenvalues Ω_B , Ω_C , and Ω_D are shown in Fig. 3 as the pulses pass through the system. If the system evolves adiabatically, it stays in the state $|\phi_D\rangle$, but the amount of support it receives from each of the states $|E_j\rangle$ will change at each avoided crossing that $|\phi_D\rangle$ encounters. In Fig. 3, there appears to be a traditional 3-level avoided crossing at about $t_{fix} \simeq 0.5 t_{tot}$. However, there are additional avoided crossings involving Ω_D that can change $|\phi_D\rangle$. In Fig. 4, we show the dependence of the three Floquet states $|\phi_B\rangle$, $|\phi_C\rangle$, and $|\phi_D\rangle$ on the energy eigenstates $|E_j\rangle$ as the pulses pass through the system. We see that $|\phi_D\rangle$ starts out fully supported by $|E_1\rangle$ then partially changes its support from $|E_1\rangle$ to $|E_{15}\rangle$ and finally, after the pulses have passed, ends with equal support from $|E_1\rangle$ and $|E_4\rangle$. State $|\phi_B\rangle$, on the other hand, begins with equal support from $|E_1\rangle$ and $|E_4\rangle$ and ends totally supported by $|E_{15}\rangle$. A truly adiabatic evolution of the pulses, which would keep the system in Floquet state $|\phi_D\rangle$ the whole time, would not accomplish our goal of transitioning the system from $|E_1\rangle$ to $|E_{15}\rangle$. The problem arises because additional avoided crossings occur that pull the system off the traditional STIRAP path. The influence of an additional small avoided crossing between Ω_B and Ω_D at about $t_{fix} = 0.55$ is clearly seen. This additional small avoided crossing is a manifestation of classical chaos in the quantum dynamics similar to the ones seen for the double well system in [10].

The dynamics can be analyzed in more detail by using the Landau-Zener formula to calculate the probability of a transition at an avoided crossing. The probability $P_{\nu,\nu'}$ for an avoided crossing between two Floquet eigenphases Ω_ν and $\Omega_{\nu'}$ to be crossed is given by [24], [25]

$$P_{\nu,\nu'} = \exp \left[-\frac{\pi(\delta\Omega_{\nu,\nu'})^2}{2\Gamma_{\nu,\nu'}} \right], \quad (9)$$

where $\delta\Omega_{\nu,\nu'}$ is the (minimum) spacing between Ω_ν and $\Omega'_{\nu'}$ at the avoided crossing and $\Gamma_{\nu,\nu'}$ is the magnitude of the *adiabatic* rate of change (slope) of the Floquet eigenphases. Thus,

$$\Gamma_{\nu,\nu'} = \frac{\bar{\Gamma}_{\nu,\nu'}}{t_{tot}} = \left| \frac{d\Omega_\nu}{dt} - \frac{d\Omega_{\nu'}}{dt} \right|, \quad (10)$$

where $\frac{d\Omega_\nu}{dt}$ is the slope of the eigenphase curve Ω_ν in the neighborhood of the avoided crossing. Equation (9) can be simplified to $P_{\nu,\nu'} = \exp[-t_{tot}\gamma_{\nu,\nu'}]$, where $\gamma_{\nu,\nu'} = \frac{\pi(\delta\Omega_{\nu,\nu'})^2}{2\Gamma_{\nu,\nu'}}$.

In order for a crossing to be traversed adiabatically, $P_{\nu,\nu'} \approx 0$, and the actual time scale of the STIRAP must be adjusted accordingly. Thus, the transfer probability $P_{\nu,\nu'}$ will be very small if $t_{tot} > 1/\gamma_{\nu,\nu'}$. For the *BD* avoided crossing, we estimate the gap $\delta\Omega_{BD}$ to be 1.984×10^{-3} , and Γ_{BD} to be 0.135, concluding that $t_{tot} > 2.184 \times 10^4$. For ^{85}Rb atoms confined in a one-dimensional optical lattice by detuning away from the D_2 transition line, the recoil frequency, ω_r is about 24 *KHz* [20]. The characteristic time scale here is $1/(4\omega_r)$, or 1.03×10^{-5} seconds. We can plug this value to the minimum value(s) of t_{tot} to get the actual time. Thus, for the ^{85}Rb atom, we get $t_{tot} > 0.225$ *sec* for the *BD* crossing. If the time scale for the stirap is faster than 0.225 seconds, then the crossing is traversed diabatically and traditional 3-level STIRAP will be seen. For ^{87}Rb atoms in the $F = 2$, $m_F = 2$ state confined in the toroidal magnetic trap of Fernholtz et al, the resonance condition, as well as one dimensional confinement, are met at a radius $\sim \mu\text{m}$ [19], and can be adjusted to replicate the time scales of the optical lattice.

We now compare the results obtained from Floquet theory to numerical simulations of the actual dynamics of the system as it evolves through time. The full multilevel Schrödinger equation for this system, starting from the undriven ground state $|\psi(0)\rangle = |E_1\rangle$, can be solved numerically for the system as it evolves from $t = 0$ to $t = t_{tot}$. The rate at which the avoided crossings are traversed can be controlled by controlling t_{tot} . Figures 5.a through 5.d show the numerical time evolution of the wavefunction of the two-boson system $|\psi(t)\rangle$, starting from the ground state $|E_1\rangle$. For small values of t_{tot} , the system traverses the *BD* avoided crossing diabatically, and a near-complete population transfer to $|E_{15}\rangle$ occurs due to the preceding 3-level avoided crossing, replicating the traditional STIRAP process. This can be seen in Figure 5.a, where $t_{tot} = 7200$. As we increase t_{tot} towards (and beyond) 2.184×10^4 , the time evolution approaches that of the Floquet state $|\phi_D\rangle$ as shown in Fig 4. Figure 5.d shows $|\psi(t)\rangle$ as it evolves in time for $t_{tot} = 90,000$. The centroids of the components $\langle E_i|\psi(t)\rangle$ are identical to the components $\langle E_i|\phi_D\rangle$ in Fig 4. The oscillations in the probability occur due to nonadiabatic effects as demonstrated by Berry [26], and decrease in amplitude as we move further into the adiabatic regime.

4 Conclusion

We have analyzed the dynamics of interacting two-boson systems for ultracold alkali metal atoms in an optical lattice with periodic boundary conditions. We have demonstrated the feasibility of a controlled excitation of the system into a higher energy state using STIRAP, induced by time dependent modulations of the optical lattice.

For sufficiently large amplitude modulations, the effects of the underlying classical dynamics [27] start to manifest themselves through small avoided crossings between the involved Floquet eigenphases. The STIRAP pulses were tuned to connect very high energy states (the final state being the fifteenth energy level). Avoided crossings between the other Floquet states connected cause the outcome to differ from traditional three level STIRAP. By traversing these additional small avoided crossings diabatically, in order to eliminate their effect on the system, we obtain the outcome expected for a three-level STIRAP process.

5 Acknowledgments

The authors wish to thank the Robert A. Welch Foundation (Grant No. F-1051) for support of this work. The authors also thank the Texas Advanced Computing Center (T.A.C.C.) at the University of Texas at Austin for the use of their high-performance distributed computing grid.

References

- [1] J. Oreg, F. T. Hioe, and J. H. Eberly, *Phys. Rev. A*, **29** 690 (1984).
- [2] F. T. Hioe, *Phys. Rev. A*, **29** 3434 (1984).
- [3] M. Becker, U. Gaubatz, P.L. Jones, and K. Bergmann, *J. Chem Phys*, **87** 5064 (1987).
- [4] J. R. Kuklinski, U. Gaubatz, F. T. Hioe, and K. Bergmann, *Phys. Rev. A*, **40** 6741 (1989).
- [5] U. Gaubatz, P. Rudecki, M. Becker, S. Schiemann, M. Kulz, and K. Bergmann, *Chem Phys Lett*, **149** 463 (1998).
- [6] Nikolay V. Vitanov, Thomas Halfmann, Bruce W. Shore, and K. Bergmann, *Annu. Rev. Phys. Chem.* **52** 763 (2001).
- [7] H.-G Rubahn, E. Konz, S. Schiemann, and K. Bergmann, *Z. Phys. D* **22** 401 (1991).
- [8] Kyungsun Na and L. E. Reichl, *Phys. Rev. A* **72** 013402 (2005).
- [9] Benjamin P. Holder and Linda E. Reichl, *Phys. Rev. A* **76** 013420 (2007)

- [10] Analabha Roy and L. E. Reichl, *Phys. Rev. A* **77** 033418 (2008).
- [11] Kyungsun Na and L. E. Reichl, *Phys. Rev. A* **70** 063405 (2004).
- [12] Phillip L. Gould, George A. Ruff, and David E. Pritchard, *Phys. Rev. Lett.* **56** 827 (1986).
- [13] C. Salomon, J. Dalibard, A. Aspect, H. Metcalf, and C. Cohen-Tannoudji, *Phys. Rev. Lett.* **59** 1659 (1987).
- [14] A. F. Bernhardt and B. W. Shore, *Phys. Rev. A* **23** 1290 (1981).
- [15] E.M. Wright and P. Meystre, *Optics Comm.* **75** 388 (1990).
- [16] R. Graham, M. Schlautmann, and P. Zoller, *Phys. Rev. A* **45** R19 (1992).
- [17] F. L. Moore, J. C. Robinson, C. Bharucha, P. E. Williams, and M. G. Raizen, *Phys. Rev. Lett.* **73** 2974 (1994).
- [18] A. Itah, H. Veksler, O. Lahav, A. Blumkin, C. Moreno, C. Gordon, and J. Steinhauer, <http://arxiv.org/abs/0903.3282>, Mar 2009.
- [19] T. Fernholtz, R. Gerritsma, P. Kruger and R.J.C. Spreeuw, *Phys. Rev. A* **75** 063406 (2007).
- [20] Daniel A. Steck, Windell H. Oskay, and Mark G. Raizen, *Science* **293** 274 (2001).
- [21] Mark Galassi, Jim Davies, J. Theiler, B. Gough, G. Jungman, M. Booth, and F. Rossi. *GNU Scientific Library Reference Manual - Second Edition*. Network Theory Ltd., 2003. Also available online at <http://www.gnu.org/software/gsl/manual/>.
- [22] J.R. Dormand and P.J. Prince, *J. Comp. Appl. Math.* **6** 19 (1980).
- [23] Vicente Hernandez, Jose Roman, Eloy Romero, Andres Tomas, and Vicent Vidal. *SLEPc Users Manual, Scalable Library for Eigenvalue Problem Computations*. Departamento de Sistemas Informaticos y Computacion, Valencia, Spain, February 2009. Also available online at <http://www.grycap.upv.es/slepc>.
- [24] G. Zener, *Proc. R. Soc. London Ser. A*, **137** 696 (1932).
- [25] Curt Wittig, *J. Phys. Chem. B* **109** 8428 (2005).
- [26] M.V. Berry, *Proc. R. Soc. London, Ser. A* **429** 61 (1990).
- [27] L.E. Reichl. *The Transition to Chaos: Conservative Classical Systems and Quantum Manifestations*. Springer Verlag, Berlin, 2 edition, 2004.

List of Figures

1	Energy curves of the first 66 lowest-energy states of both even and odd parities for the two-boson system. (a) The energy levels plotted as a function of κ_0 for interaction amplitude $u_0 = 23.0$. The region of interest is highlighted by a box. (b) Magnified view of the region of interest boxed in Fig. 1.a. The levels being connected by STIRAP for this particular value of κ_0 are indicated. The value of κ_0 has been adjusted so that $\frac{\omega_f}{\omega_s} = \frac{3}{2}$	10
2	Wavefunction plots for states (a) $ E_1\rangle$, (b) $ E_3\rangle$, (c) $ E_4\rangle$, (d) $ E_5\rangle$, (e) $ E_{15}\rangle$	11
3	Floquet quasienergies Ω_ν as a function of adiabatic time t_{fix}/t_{tot} for $\lambda^0 = 0.2$. The labels Ω_B , Ω_C , and Ω_D denote the floquet quasienergy curves corresponding to the Floquet eigenstates $ \phi_B\rangle$, $ \phi_C\rangle$, and $ \phi_D\rangle$, respectively.	12
4	Plot of the Floquet eigenfunctions in the undriven Hamiltonian representation ($\langle E_i \phi_{B-D} \rangle$). The components of the Floquet states in each energy level are numbered. Note the influence of the avoided crossings in $ \phi_D\rangle$	13
5	Plots of $ \langle E_j \psi(t) \rangle ^2$ as a function of time of the system as it evolves under the influence of STIRAP pulses from the ground state $ \psi(0)\rangle = E_1\rangle$ for different values of t_{tot} . All units are dimensionless. (a) $t_{tot} = 7200$. (b) $t_{tot} = 12,000$. (c) $t_{tot} = 24,000$. (d) $t_{tot} = 90,000$	14

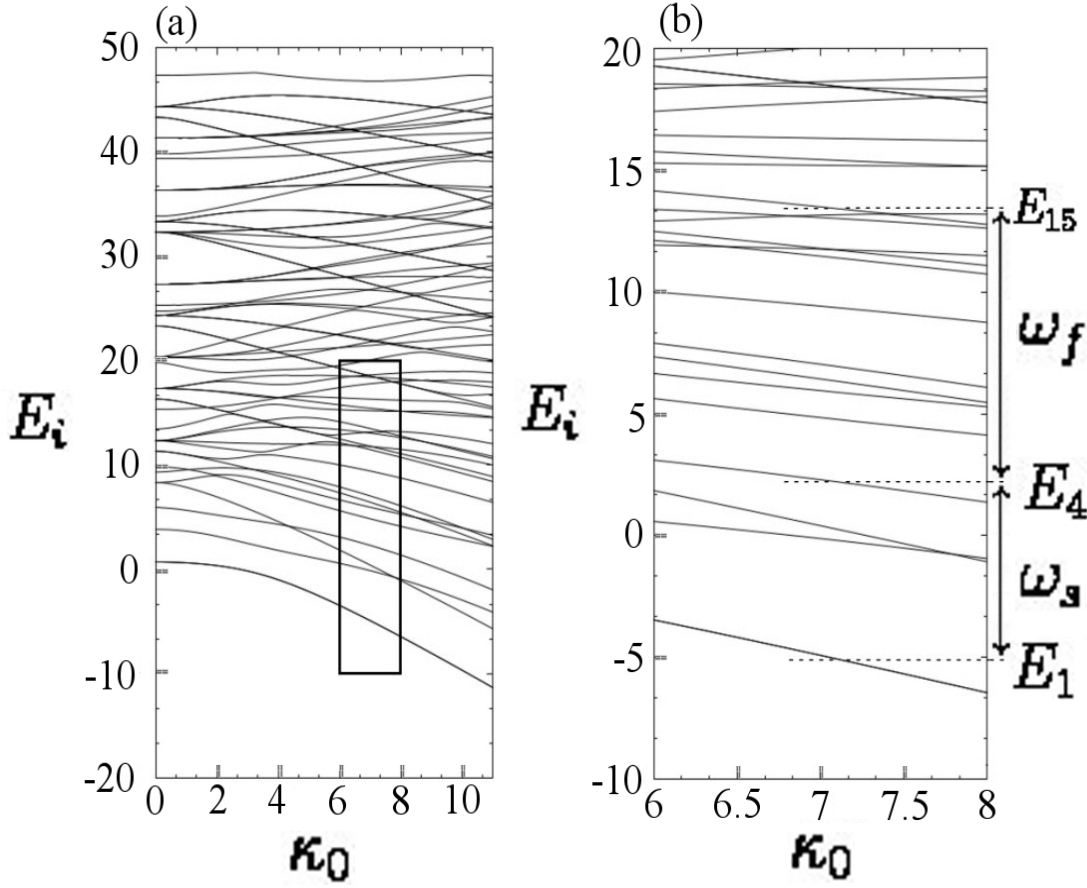


Figure 1: Energy curves of the first 66 lowest-energy states of both even and odd parities for the two-boson system. (a) The energy levels plotted as a function of κ_0 for interaction amplitude $u_0 = 23.0$. The region of interest is highlighted by a box. (b) Magnified view of the region of interest boxed in Fig. 1.a. The levels being connected by STIRAP for this particular value of κ_0 are indicated. The value of κ_0 has been adjusted so that $\frac{\omega_f}{\omega_s} = \frac{3}{2}$.

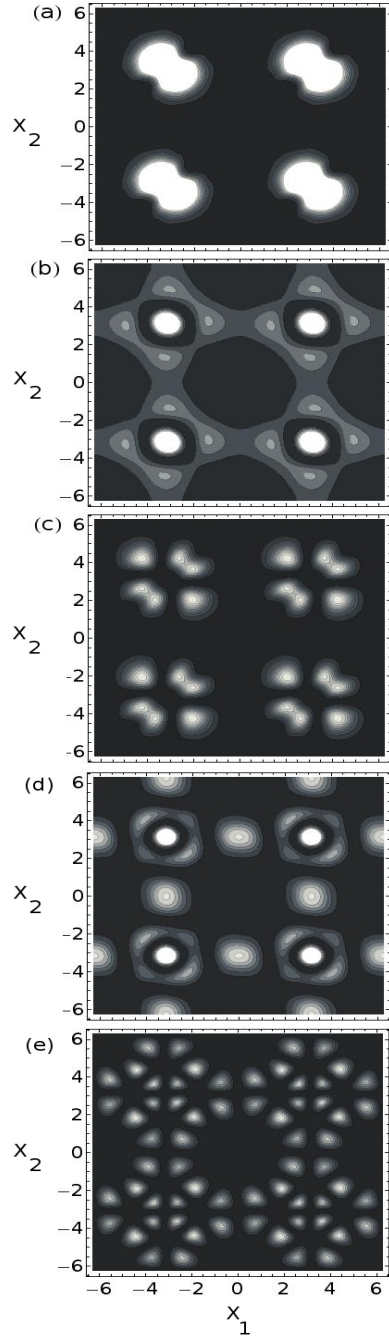


Figure 2: Wavefunction plots for states (a) $|E_1\rangle$, (b) $|E_3\rangle$, (c) $|E_4\rangle$, (d) $|E_5\rangle$, (e) $|E_{15}\rangle$.

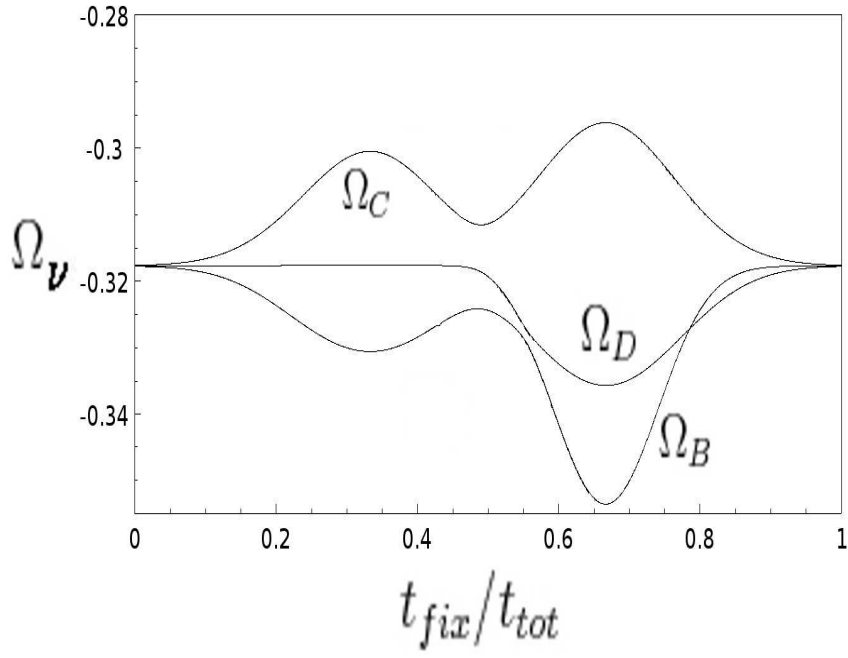


Figure 3: Floquet quasienergies Ω_ν as a function of adiabatic time t_{fix}/t_{tot} for $\lambda^0 = 0.2$. The labels Ω_B , Ω_C , and Ω_D denote the floquet quasienergy curves corresponding to the Floquet eigenstates $|\phi_B\rangle$, $|\phi_C\rangle$, and $|\phi_D\rangle$, respectively.

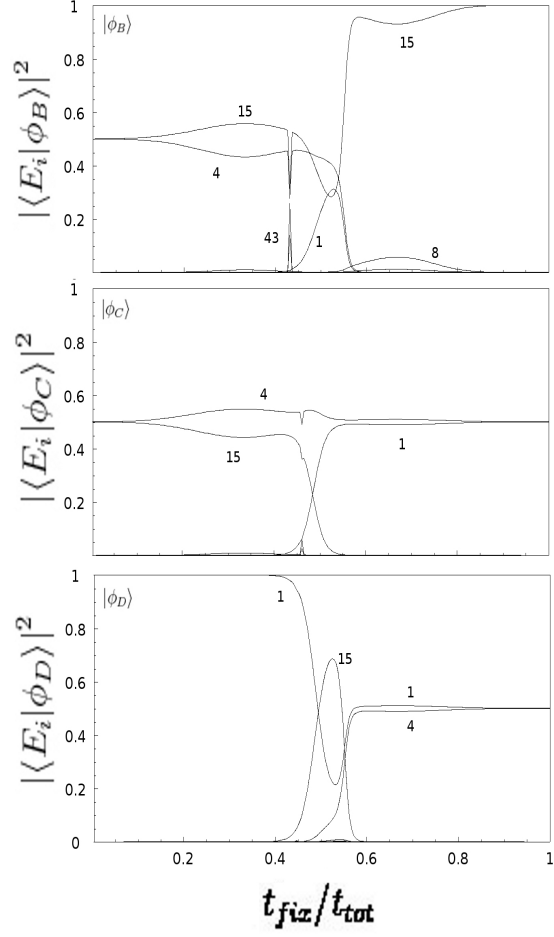


Figure 4: Plot of the Floquet eigenfunctions in the undriven Hamiltonian representation ($\langle E_i | \phi_{B-D} \rangle$). The components of the Floquet states in each energy level are numbered. Note the influence of the avoided crossings in $|\phi_D\rangle$.

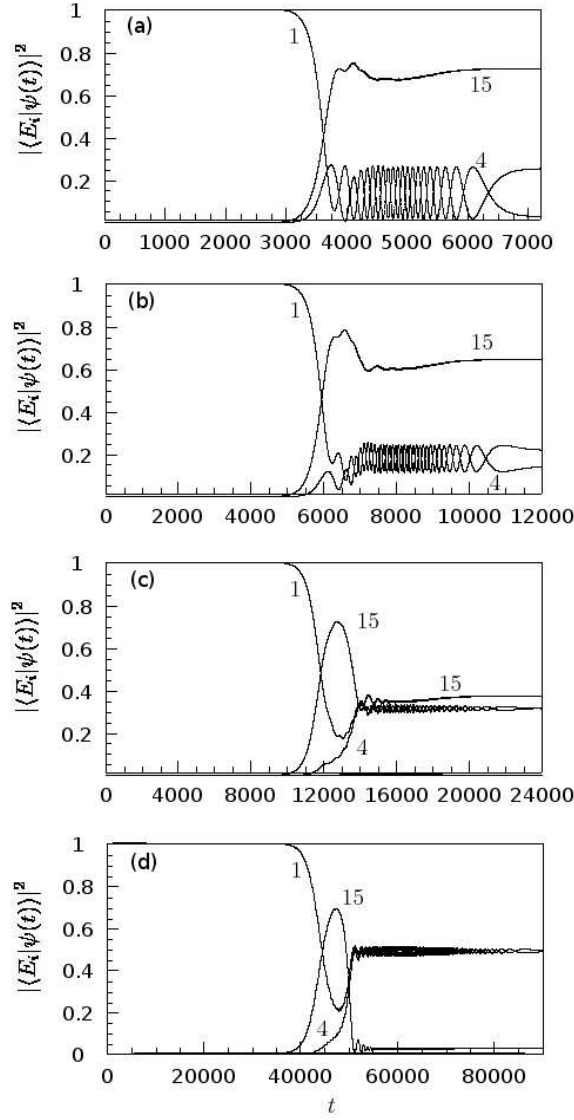


Figure 5: Plots of $|\langle E_j | \psi(t) \rangle|^2$ as a function of time of the system as it evolves under the influence of STIRAP pulses from the ground state $|\psi(0)\rangle = |E_1\rangle$ for different values of t_{tot} . All units are dimensionless. (a) $t_{tot} = 7200$. (b) $t_{tot} = 12,000$. (c) $t_{tot} = 24,000$. (d) $t_{tot} = 90,000$.